PROCEEDINGS OF SCIENCE

# Highlights of LHC experiments - part II

**Tiziano Camporesi**
*CERN*
*E-mail:* tiziano.camporesi@cern.ch

This paper describes a selection of results contributed to the ICHEP conference by the CMS and ALICE collaborations, operating at the CERN LHC. The LHC accelerator has been operating at a proton–proton collision energy of 13 TeV since 2015 and its performance has been outstanding in 2016, having provided 13 $fb^{-1}$ of data that could be analysed in time for the conference. Given the large amount of contributions (CMS alone submitted more than 70 new results) only a selection of them will be mentioned. Our choice of measurements shows the sophistication of the detectors and how we explore the complexity of the Standard Model; and since we are exploring a new energy domain, we will also cover a selection of searches for supersymmetry and other topics beyond the Standard Model. We finish with a selection of recent results from the Heavy Ion program.

*38th International Conference on High Energy Physics*
*3-10 August 2016*
*Chicago, USA*





PoS(ICHEP2016)005

## 1. Introduction

The LHC accelerator restarted in 2015 providing proton-proton collisions at the new record energy of 13 TeV. The performance of the accelerator has been steadily improving, reaching its design luminosity during the 2016 campaign. CMS has contributed to this conference more than 70 new results based on the luminosity collected in 2015 ($3.6\times\text{fb}^{-1}$) and in the first phase of the 2016 data taking campaign ($12.9\,\text{fb}^{-1}$). The extraordinary performance of the accelerator has been matched by CMS, which has collected data with 95% efficiency, and the quality of the data collected is such that more than 92% is usable for the physics analyses. In preparation for the 2016 run, strategies and algorithms were developed to mitigate the effects of pileup; the number of concurrent pp collisions per bunch crossing has averaged 25, with tails exceeding 50. The overall performance of CMS benefited from the introduction of the upgraded first level trigger, operational from the start of the 2016 run and performing according to expectations, with remarkable improvements in tau triggering efficiency and improved shower localisation and energy resolution for the calorimeter triggers.

## 2. Standard Model measurements

CMS contributed 16 new Standard Model (SM) measurements, ranging from jet physics to electroweak boson production. Among many new measurements involving final states with top quarks, we highlight the measurement of the $\mathrm{t\bar{t}}$ production cross section at $\sqrt{s} = 13\,\text{TeV}$, using 2015 data corresponding to an integrated luminosity of $2.3\,\text{fb}^{-1}$. Final states including one isolated charged lepton (electron or muon) and at least one jet are selected and categorized according to the multiplicity of jets. From a likelihood fit to the invariant mass of the isolated lepton and a jet identified as stemming from the fragmentation and hadronization of a b quark, the cross section is measured to be $\sigma(\mathrm{t\bar{t}}) = 834.6 \pm 2.5\ (\text{stat}) \pm 22.8\ (\text{syst}) \pm 22.5\ (\text{lumi})$ pb, in agreement with the SM prediction. Using the expected dependency of the cross section on the top quark pole mass, the latter is extracted to be $m_{\mathrm{t}} = 172.3^{+2.7}_{-2.3}$ GeV. Figure 1-left shows this result together with previous measurements.

The cross section for the production of single top quarks in the $t$ channel was also measured with the 2015 dataset [3]. The event selection requires one muon and two jets, where one of the jets is identified as originating from a bottom quark. Several kinematic variables are then combined into a multivariate discriminator to distinguish signal from background events. A fit to the distribution of the discriminating variable yields a total cross section of $232 \pm 13(\text{stat}) \pm 28(\text{syst})$ pb and a ratio of top quark and top antiquark production of $R_{t\text{-ch.}} = 1.81 \pm 0.18(\text{stat}) \pm 0.15(\text{syst})$. From the total cross section, the absolute value of the CKM matrix element $V_{\mathrm{tb}}$ is calculated to be $1.03 \pm 0.07(\text{exp}) \pm 0.02(\text{theo})$. These results are in agreement with the SM expectations. Figure 1-right shows this result, as well as previous measurements.

The 2016 data provided a measurement of the cross section of top quark pairs produced in association with a W or Z boson [4]. The measurement is performed in same-sign dilepton, three- and four-lepton final states, where the jet and b-jet multiplicities are exploited to enhance the signal-to-background ratio. The $\mathrm{t\bar{t}W}$ and $\mathrm{t\bar{t}Z}$ production cross sections are, respectively, $\sigma(\mathrm{t\bar{t}Z}) = 0.70^{+0.16}_{-0.15}(\text{stat})^{+0.14}_{-0.12}(\text{syst})$ pb and $\sigma(\mathrm{t\bar{t}W}) = 0.98\ ^{+0.23}_{-0.22}(\text{stat})\ ^{+0.22}_{-0.18}(\text{syst})$ pb, with an expected (observed) significance of 2.6 (3.9) and 6.0 (4.4) standard deviations from the background-only hypothesis. Also in this case the result is in agreement with the SM expectations.

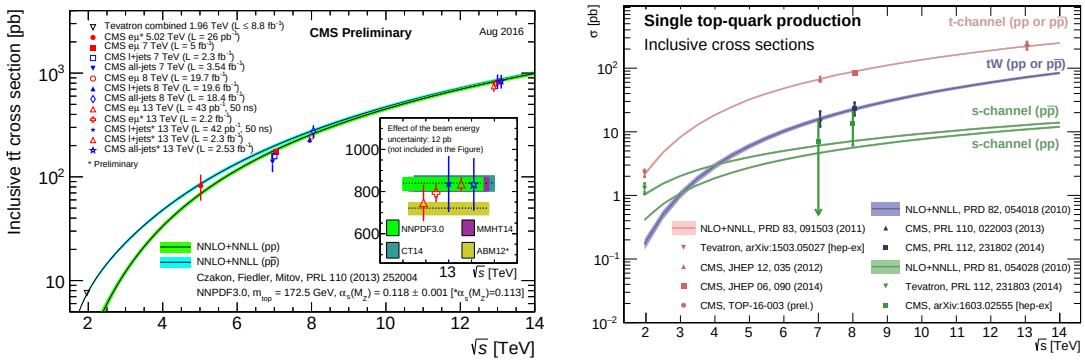


**Figure 1:** Left: Top quark pair cross section summary of most precise CMS measurements in the dilepton and l+jets channel in comparison with the theory calculation at NNLO+NNLL accuracy. The Tevatron measurements are also shown. Right: Summary of single top cross section measurements by CMS, as a function of centre-of-mass energy.

## 3. Higgs physics

CMS contributed to this conference 13 new results related to Higgs measurements or searches, among which we highlight the observation of the Higgs boson decaying to ZZ and to two photons. With the 12.9 fb$^{-1}$ of luminosity collected in 2016, CMS studied the properties of the Higgs boson sing the $\mathrm{H} \to \mathrm{ZZ} \to 4\ell$ ($\ell = \mathrm{e}, \mu$) decay channel. The observed significance for the standard model Higgs boson with $m_{\mathrm{H}} = 125.09$ GeV is $6.2\sigma$, where the expected significance is $6.5\sigma$. The signal strength modifier $\mu$ relative to the standard model expectation is $\mu = 0.99^{+0.33}_{-0.26}$ at $m_{\mathrm{H}} = 125.09$ GeV. The signal-strength modifiers for the main Higgs boson production modes have also been constrained. The model-independent fiducial cross section is $2.29^{+0.74}_{-0.64}(\mathrm{stat})^{+0.30}_{-0.23}(\mathrm{syst})^{+0.01}_{-0.05}(\mathrm{model\ dep.})$ fb, to be compared to the SM expectation $\sigma^{\mathrm{SM}}_{\mathrm{fid.}} = 2.53 \pm 0.13$ fb. The measured mass is $m_{\mathrm{H}} = 124.50^{+0.48}_{-0.46}$ GeV and the width is constrained to be $\Gamma_{\mathrm{H}} < 41$ MeV comparing the on-peak with the off-peak rates.

In the two photon decay channel [6], using the the 2016 luminosity, the Higgs boson is observed at the Run 1 ATLAS+CMS combined $m_H = 125.09$ GeV with a significance of 5.6 $\sigma$, where 6.2 $\sigma$ is expected, see Figure 3(b). A maximum significance of 6.1 $\sigma$ is observed at 126.0 GeV. The best-fit signal strength relative to the standard model prediction is $0.95 \pm 0.20 = 0.95 \pm 0.17(\mathrm{stat})^{+0.10}_{-0.07}(\mathrm{syst})^{+0.08}_{-0.05}(\mathrm{th})$ when the mass parameter is profiled in the fit, and $0.91 \pm 0.20 = 0.91 \pm 0.17(\mathrm{stat})^{+0.09}_{-0.07}(\mathrm{syst})^{+0.08}_{-0.05}(\mathrm{th})$ when it is fixed to $m_H = 125.09$ GeV. The search for the associated production of a standard model Higgs boson and a top quark-anti quark pair ($\mathrm{t\bar{t}H}$) has been performed using the data collected in 2015 and 2016 [7]. The analysis uses

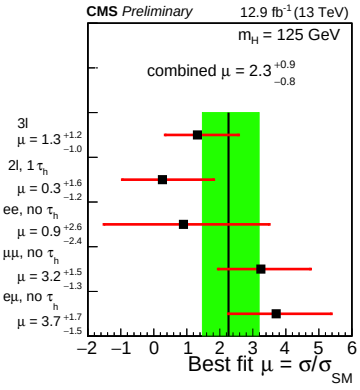


**Figure 2:** Best fit signal strength for the 2016 analysis alone, in the dilepton and trilepton channels.

events with two leptons of the same charge or at least three charged leptons, produced together with b jets, targeting Higgs boson decay modes to WW$^*$, ZZ$^*$ and $\tau\tau$, and leptonic decays of at least one of the top quarks. The combination, see Figure 2, yields a $t\bar{t}H$ signal strength of $2.0^{+0.8}{}_{-0.7}$ times the standard model prediction. This is used to set a 95% confidence level upper limit on the signal production cross section of 3.4 times the standard model expectation, compared to an expected upper limit of $1.3^{+0.6}{}_{-0.4}$ in the absence of a signal.

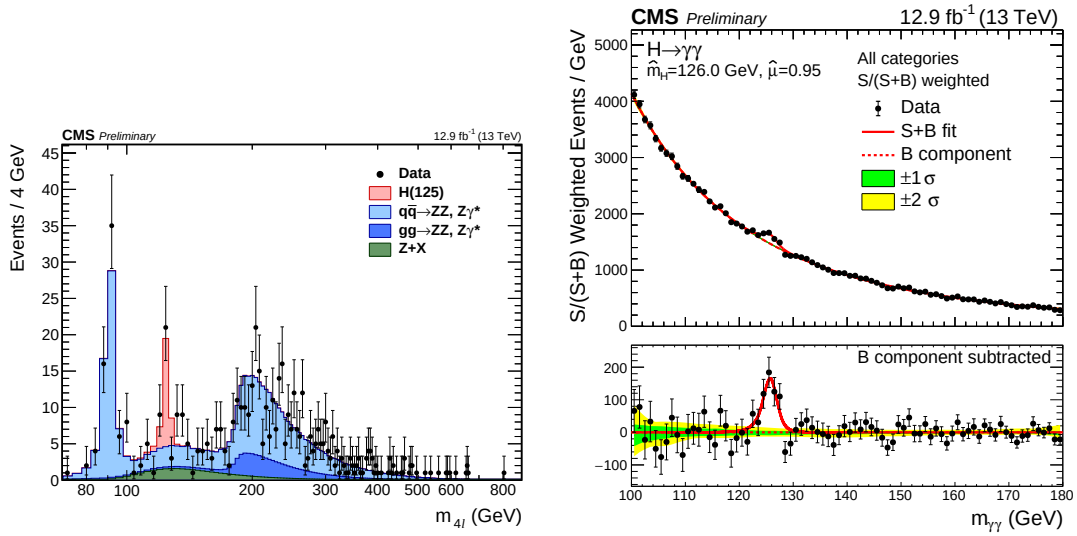


(a) (b)

**Figure 3:** Right: Distribution of the four-lepton reconstructed invariant mass $m_{4l}$ in the full mass range. Points with error bars represent the data and stacked histograms represent expected distributions. Left: Distribution of the invariant mass of the two photon decay channel analysis. Data points (black) and signal plus background model fits for all categories summed with the categories summed weighted by their sensitivity. The insert at the bottom shows the residuals after background subtraction.

## 4. Beyond the Standard Model: exotic searches

CMS has contributed to this conference 28 new results related to searches related to exotic scenarios of physics beyond the Standard Model. A result which has received a lot of attention is the search for the resonant production of high-mass photon pairs, specifically spin-0 and spin-2 resonances with an invariant mass between 0.5 and 4.5 TeV, and with a width, relative to the mass, between $1.4\times10^{-4}$ and $5.6\times10^{-2}$ [8]. The data sample corresponds to an integrated luminosity of $12.9\,\text{fb}^{-1}$ of proton-proton collisions collected in 2016. No significant excess is observed relative to the standard model expectation. The results of the search are combined statistically with those previously obtained in 2012 and 2015 at $\sqrt{s}=8$ and 13 TeV, respectively (Figure 4), corresponding to integrated luminosities of 19.7 and $3.3\,\text{fb}^{-1}$, to derive exclusion limits on scalar resonances produced through gluon-gluon fusion, and on Randall–Sundrum gravitons. The lower mass limits for Randall–Sundrum gravitons range from 1.95 to 4.45 TeV for coupling parameters between 0.01 and 0.2.

A search for narrow resonances decaying to dijet final states has been performed based on the 2016 data [9]. The dijet mass spectra are well described by a smooth parameterization and no

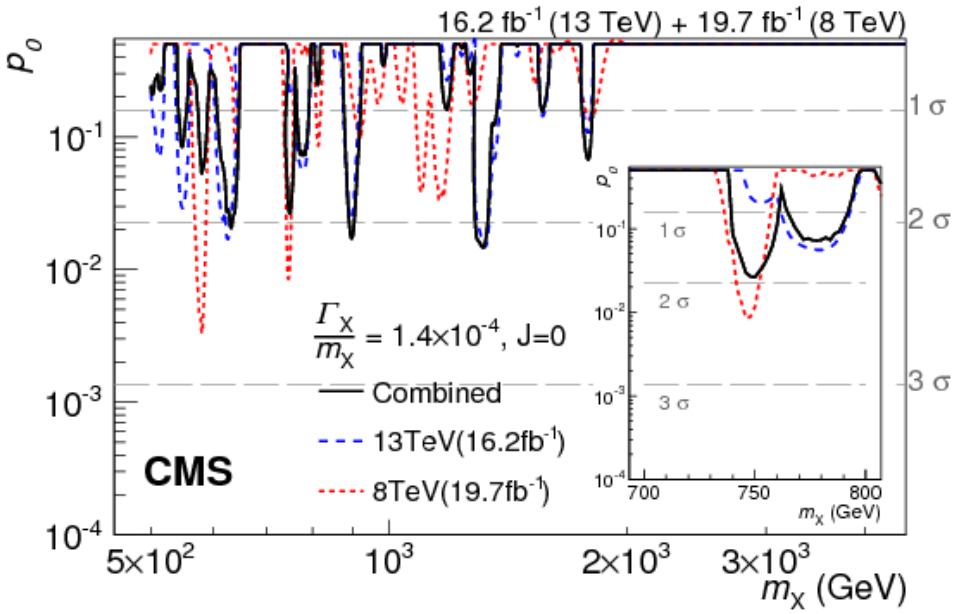


**Figure 4:** Observed background-only p-values for resonances with various $\Gamma_{PX}/m_{PX}$ as a function of the resonance mass $m_{PX}$, from the combined analysis of the 8 and 13 TeV data. The results obtained for the two individual center-of-mass energies are also shown. The insets show an expanded region around $m_{PX} =$ 750 TeV.

significant evidence for new particle production is observed. Upper limits at 95% confidence level are set on the production cross section for narrow resonances with masses above 0.6 TeV. When interpreted in the context of specific models, the limits exclude string resonances with masses below 7.4 TeV, scalar diquarks below 6.9 TeV , axigluons and colorons below 5.5 TeV, excited quarks below 5.4 TeV, color-octet scalars below 3.0 TeV, W′ bosons below 2.7 TeV, Z′ bosons below 2.1 TeV and between 2.3 to 2.6 TeV, a dark matter mediator below 2.0 TeV, and RS gravitons below 1.9 TeV, extending previously published limits in the dijet channel(Figure 5).

A search for new narrow resonances in dielectron and dimuon spectra is performed using the 2016 data [10]. The integrated luminosity corresponds to 12.4 $fb^{-1}$ and 13.0 $fb^{-1}$ for the dielectron and dimuon samples, respectively. No significant deviations from the standard model expectation are observed. Upper bounds up to 4 TeV are set on the masses of hypothetical particles that arise in new-physics scenarios.

CMS is exploring systematically the possible productions of dark matter candidates [11]. No significant excess has been observed and the results are interpreted taking into account not only the mass of the Dark Matter particle, but also of the mass of the mediator,and its coupling to the Dark matter particle on one side and the stdanrda model particle on the other side. In order to summarize the variety of results, the Figure 7 shows, for each analysis, the maximum limit on the mass of the Dark matter particle and the mediator.

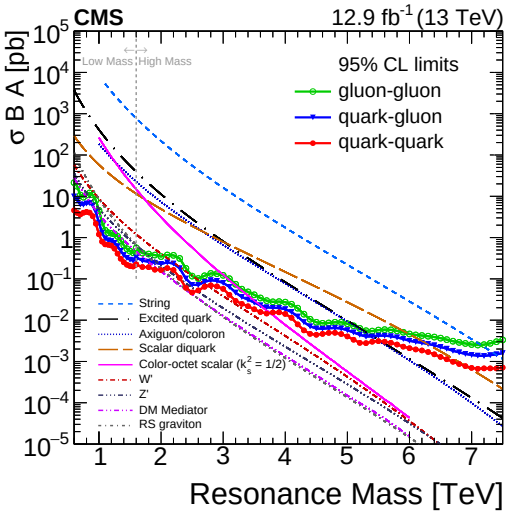


**Figure 5:** Limits from both the low-mass and high-mass search. The observed 95% CL limits (solid) are presented from the low mass search and from the high mass search (masses $\geq 1.6 TeV$). Limits are compared to the predicted cross sections of string resonances, excited quarks, axigluons, colorons, scalar diquarks, color-octet scalars, new gauge bosons, and RS gravitons.

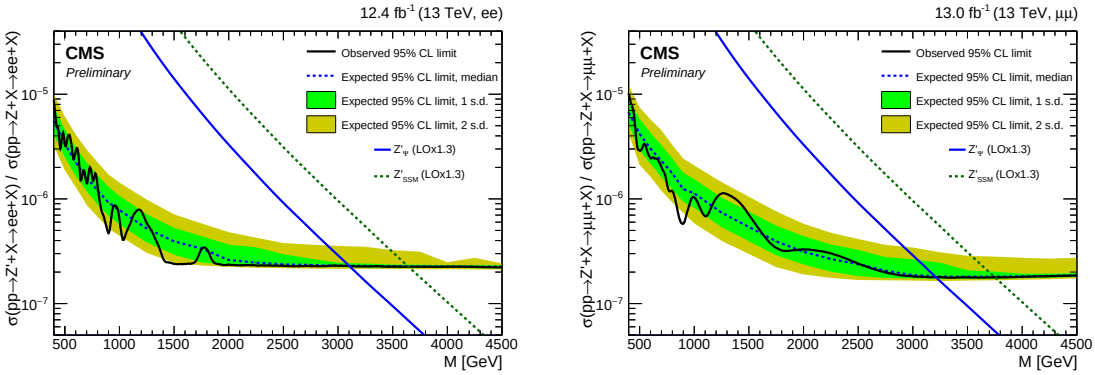


(a) (b)

**Figure 6:** The 95% CL upper limits on the production cross section times branching fraction for a spin-1 resonance with a width equal to 0.6% of the resonance mass, relative to the production cross section times branching fraction for a Z boson, for the (left) dielectron and (right) dimuon channel. The shaded bands correspond to the 68 and 95% quantiles for the expected limits. Theoretical predictions for the spin-1resonances are shown for comparison.

## 5. Beyond the Standard Model: Supersymmetry searches

CMS has contributed to this conference 16 new results related to searches related to Supersymmetric scenarios of physics beyond the Standard Model. Searches for Supersymmetric particle production have been performed with the data collected at 13 TeV, looking for final states with multileptons. Such searches can be separated into strong and electroweak production mechanisms. For the strong production mechanism ( [12])32 search regions have been used defined by the number of b-tagged jets, missing transverse energy, hadronic transverse energy, and the invariant mass

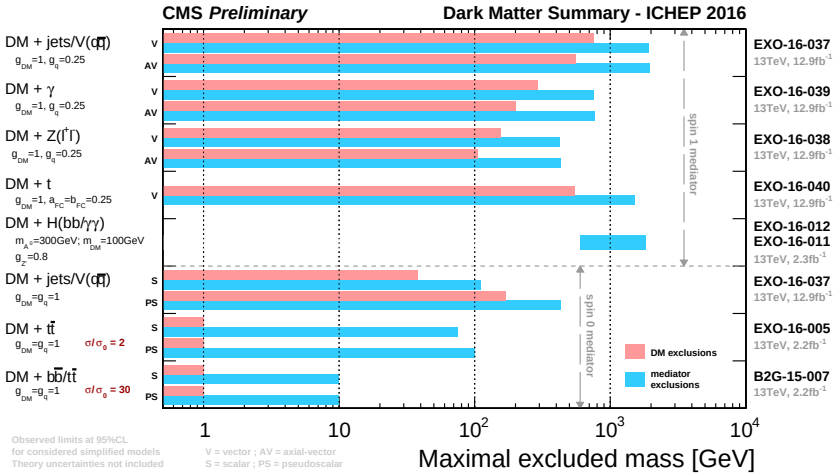


**Figure 7:** Summary of all Dark Matter Searches: in blue the max limits on mediator search decaying to dark matter (max limits on Dark matter mass in red). The plot is split by spin 0 and spin 1 and shows the assumed coupling of the mediator to Dark matter and standard model particle

of opposite-sign, same-flavor dilepton pairs in the events. No significant excess above the standard model background expectation is observed. We can then proceed to set limits for some specific simplified models: one known as T1tttt:consisting in a gluino-pair production where each gluino decays to a $t\bar{t}$ pair and an LSP. Another model containing gluino-pair production where each gluino decays to a pair of quarks and a neutralino or chargino and that neutralino or chargino then decays to a W or Z boson and an LSP, depending on the charge, is called T5qqqqVV. The Figures 8(a) and 8(b) represent the excluded regions.

Searches for the direct electroweak production of supersymmetric charginos and neutralinos hjave been perfromed selecting final states with two light leptons of the same charge and with three or more leptons including up to two hadronically decaying taus. The search was performed in 132 separate search regions depending on the number of jets, number of b-tagged jets, Number of leptons, their flavor and charge. The observed event rates are in agreement with expectations from the standard model. These results probe charginos and neutralinos with masses up to 400-1000 GeV depending on the assumed model parameters.

## 6. Heavy Ion physics

The CMS collaboration has contributed to this conference 6 results related to studies of the data obtained at LHC using Lead Ion beams. We have selected two recent results.

$D^0$ meson production has been measured in pp and PbPb collisions at $\sqrt{s_{\mathrm{NN}}} = 5.02$ TeV in the central rapidity, $|y| < 1$ , and in the transverse momentum range between 2 and 100 GeV/$c$ with the CMS detector at the LHC. The proton-proton dataset used for this analysis corresponds to an integrated luminosity of 25.8 pb$^{-1}$, while the PbPb dataset corresponds to 404 $\mu$b$^{-1}$. The measured $D^0$ spectrum in pp collisions is well described by perturbative QCD calculations. The nuclear modification factor $R_{AA}$, defined as the ratio between the corrected PbPb yield and the proton-proton cross-section scaled by the number of incoherent nucleon-nucleon collisions, was also measured.

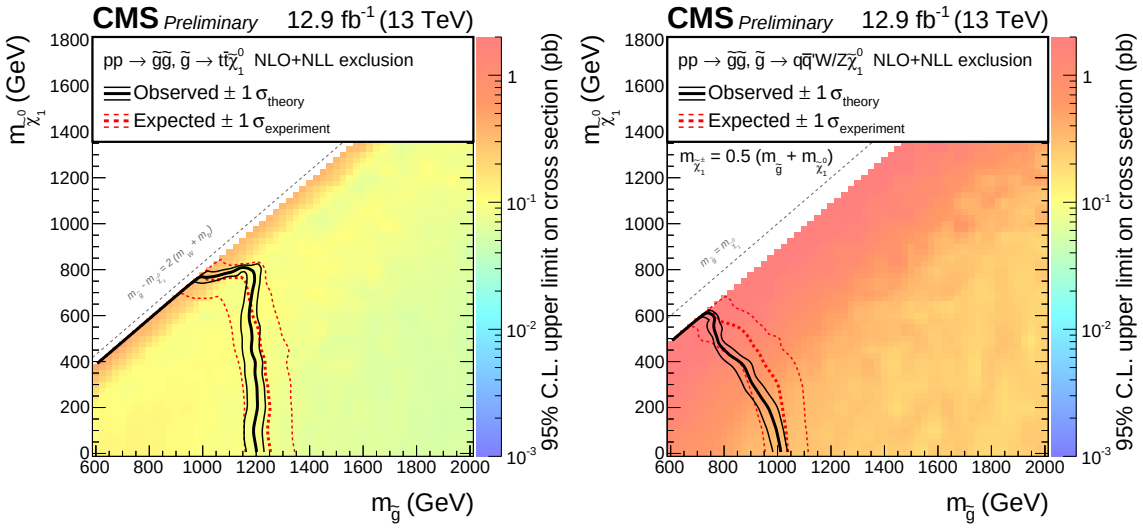


(a) (b)

**Figure 8:** Excluded region at 95% confidence in the $m(\widetilde{\chi}^0)$ versus $m(\widetilde{g})$ plane for the T1tttt (a) and for the T5qqqqWZ (b) simplified model. The color scale indicates the excluded cross section at a given point in the mass plane. The excluded regions are to the left and below the observed and expected limit curves.

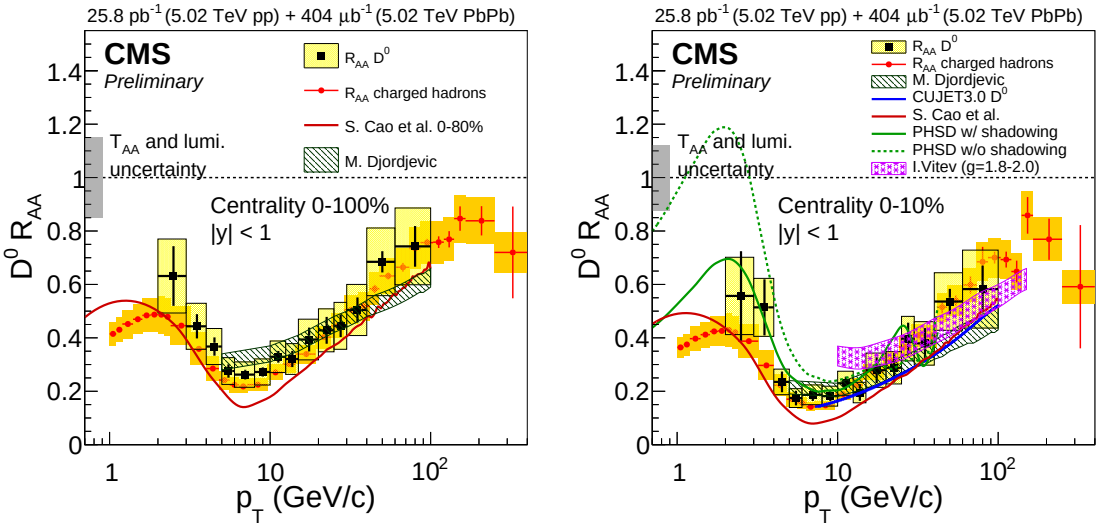


**Figure 9:** Nuclear modification factor $R_{AA}$ as a function of $p_T$ in the centrality range 0-100% (left) and 0-10% (right). The inclusive charged particle $R_{AA}$ results are superimposed for equivalent event selections [14]. The $D^0$ $R_{AA}$ are also compared to the predictions from various theoretical calculations.

In the transverse momentum range $p_T$ = 6-10 GeV/$c$, the $D^0$ yield in the PbPb collisions is suppressed by a factor of 4-5 compared to the scaled proton-proton reference. At high $p_T$, the suppression is significantly reduced, approaching roughly a factor of 1.5 for particles with $p_T$ in the range 60-100 GeV/$c$. The measured $D^0$ nuclear modification factor is compatible with the charged particle $R_{AA}$, within the experimental uncertainties. CMS has presented a measurement of the split-

ting function in pp and PbPb collisions at a center of mass energy of 5.02 TeV per nucleon pair. The virtuality evolution of partons traversing the hot QCD medium created in a heavy ion collision

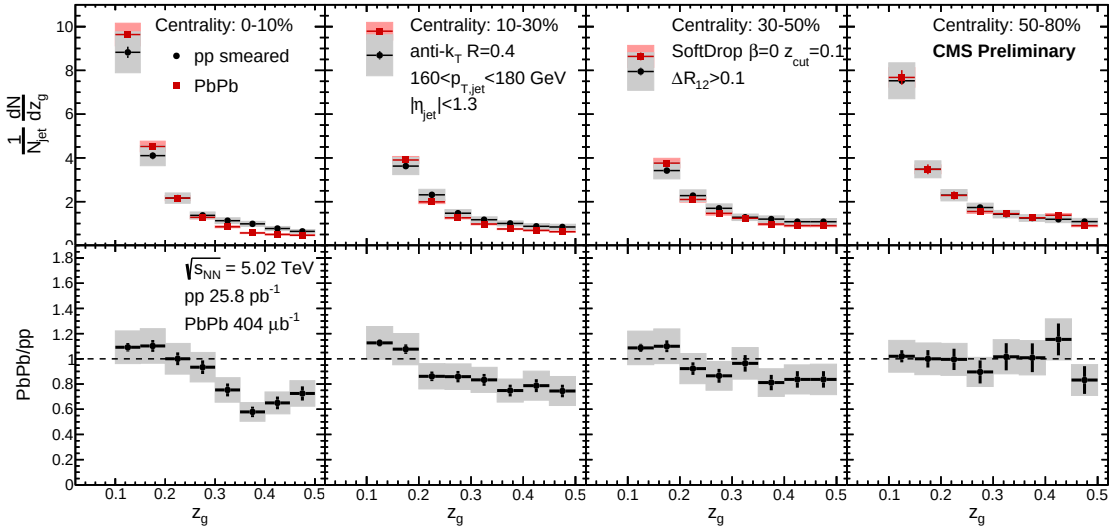


**Figure 10:** Splitting function in PbPb for $160 < p_{\mathrm{T,jet}} < 180$ GeV in several centrality ranges compared to pp data. For this comparison the resolution of the pp data is deteriorated to the same resolution as the PbPb measurement for each centrality selection. The shaded area around the data points indicates the systematic uncertainty while the vertical lines represent the statistical uncertainty.

is potentially modified due to interactions with the color charges of the medium. This measurement probes this phenomenon by measuring the generalized fragmentation function, or splitting function, over a wide range of jet transverse momentum and various collision centrality selections. The shared momentum fraction of two subjets resulting from a parton splitting is observed to be modified towards a more imbalanced fraction in central PbPb collisions compared to peripheral PbPb and pp collisions as shown in Figure 10

The ALICE collaboration has contributed 6 presentations and 2 posters related to studies of the data obtained at LHC using lead ion beams. We have selected a couple of important results of the elliptic flow parameter as a function of energy and the measurement of the $J/\psi$ nuclear modification factor at low transverse momentum in collisions of lead ions with a centre-of-mass energy $\sqrt{s_{NN}} = 5.02$ TeV per nucleon pair.

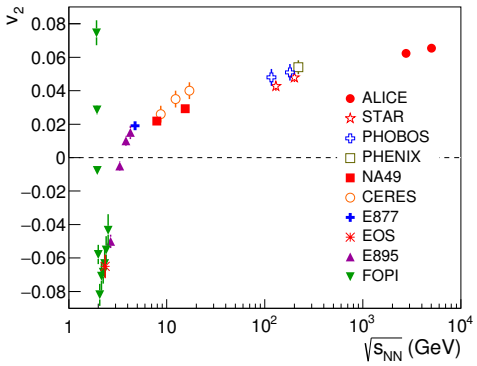


**Figure 11:** Collision energy dependence of the elliptic flow $v_2$, which measures the azimuthal asymmetry of the particle emission. [15]

One of the key measurements in heavy ion collisions are the harmonic coefficients $v_n$ of the azimuthal anisotropy of particle production. The anisotropy of final state particle production is driven

by pressure gradients in the collision system which originate from asymmetries in the initial overlap between the colliding nuclei. This process can be quantitatively modelled using a geometrical model of the initial overlap and a hydrodynamic description of the subsequent evolution of the system, which behaves as an almost ideal liquid, see e.g.[17] for a more detailed discussion.

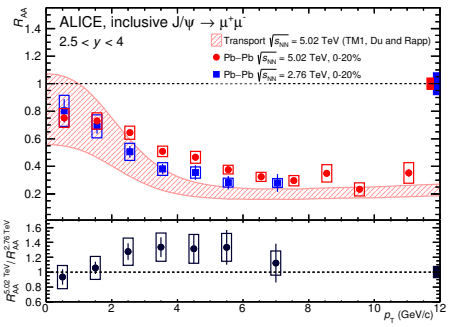


**Figure 12:** Nuclear modification factor $R_{AA}$ for $J/\psi$ production in central Pb–Pb collisions at $\sqrt{s_{NN}} = 2.76$ TeV and $\sqrt{s_{NN}} = 5.02$ TeV [16]. The band indicates a model including $J/\psi$ dissociation and regeneration by recombination of independently produced charm quarks. [22]

Figure 11 shows the dependence of the elliptic flow coefficient $v_2$ on the collision energy. The increase of $v_2$ with collision energy at high energies is due to the increasing initial temperature and the longer duration of the expansion and cool-down of the system [17]. The latest measurements using run-2 data with a collision energy $\sqrt{s_{NN}} = 5.02$ TeV follows the trend, indicating that the initial temperature and density are slightly higher at the run-2 collision energy than at the lower run-1 energy $\sqrt{s_{NN}} = 2.76$ TeV. Figure 12 shows the nuclear modification factor for $J/\psi$ production in Pb–Pb collisions as a function of transverse momentum for two collision energies. The nuclear modification factor is the ratio of production cross sections in nuclear collisions and proton-proton collisions, scaled by the number of binary collisions in the nuclear collision. The nuclear modification factor is unity when particle production in nuclear collisions is like an independent superposition of nucleon-nucleon collisions. The observed suppression ($R_{AA} < 1$) is attributed to melting of the excited charmonium states in the Quark Gluon Plasma that is produced in the collision. At LHC energies, the $R_{AA}$ increases at low $p_T$, which is thought to be due to formation of $J/\psi$ mesons from the recombination of charm quarks from independently produced pairs of charm quarks (several charm quark pairs are produced in each collision at the LHC). This effect has not been seen at the lower RHIC energies ($\sqrt{s_{NN}} = 200$ Gev). The new result for $R_{AA}$ at run-2 energies is slightly above the run-1 results, which is in line with expectations from various models, which take into account the increase of the charm production cross section and the change in the transverse momentum distributions [23, 22, 21, 20, 19].

## 7. Conclusions

The LHC is now is now in production mode at collision energies of 13 TeV: the original performance parameters have been exceeded and the early part of the 2016 run shows that the goals set for the overall program are well within reach. The accelerator performance is matched by the experiments: CMS has presented to this conference more than 70 new results. The Higgs boson is now a matter of research and most of the Run1 limits have been improved. The Heavy ion program is also achieving new and interesting results which shed new light on the behaviour of the quark gluon plasma.

**References**


[1] The CMS Collaboration, *The CMS experiment at the CERN LHC*, JINST 3 S08004 (2008), http://iopscience.iop.org/1748-0221/3/08/S08004/

[2] The CMS collaboration, CMS PAS TOP-16-006, *Inclusive ttbar cross section in the l+jets channel at 13 TeV*

[3] The CMS collaboration, CMS PAS TOP-16-003, *Inclusive single top cross section in t-channel at 13 TeV*

[4] The CMS collaboration, CMS PAS TOP-16-017, *Measurement of the top pair-production in association with a W or Z boson in pp collisions at 13 TeV*

[5] The CMS collaboration, CMS PAS HIGGS-16-033, *Measurements of properties of the Higgs boson and search for an additional resonance in the four-lepton final state at sqrts = 13 TeV*

[6] The CMS collaboration, CMS PAS HIGGS-16-020, *Higgs to gammagamma measurements at 13 TeV using 2016 data*

[7] The CMS collaboration, CMS PAS HIGGS-16-022, *Search for the ttH process with multilepton decays using the 2016 data*

[8] The CMS collaboration, CMS PAS EXO-16-027, *Search for high-mass resonances in diphoton final state using 2016 data*

[9] The CMS collaboration, CMS PAS EXO-16-032, *Search for high-mass resonances in dijet final state with 2016 data*

[10] The CMS collaboration, CMS PAS EXO-16-031, *Search for high-mass resonances in dilepton final state with 2016 data*

[11] The CMS collaboration, CMS PAS EXO-16-037, *Search for dark matter in jets+MET final state with 2016 data*
CMS PAS EXO-16-039, *Search for dark matter in photon+MET final state with 2016 data*
CMS PAS EXO-16-038, *Search for dark matter in Z(ll) MET final state using the 2016 dataset*
CMS PAS EXO-16-040, *Search for dark matter in top+MET final state with 2016 data*
CMS PAS EXO-16-012, *Search for dark matter in H(bb)+MET channel*
CMS PAS EXO-16-011, *Search for dark matter in H(gammagamma)+MET channel*
CMS PAS EXO-16-005, *Search for dark matter in association with a top quark pair*
CMS PAS B2G-15-007, *Search for Dark Matter with b quarks*

[12] The CMS collaboration, CMS PAS SUS-16-022, *Search for SUSY with multileptons in 13 TeV data*

[13] The CMS collaboration, CMS PAS EXO-16-024, *Search for electroweak SUSY production in multi-lepton final state at 13 TeV*

[14] The CMS collaboration, CMS-HIN-15-015, *Charged Particle Nuclear Modification Factors in PbPb collisions at 5 TeV*

[15] The ALICE collaboration, *Anisotropic flow of charged particles in Pb-Pb collisions at* $\sqrt{s_{\rm NN}} = 5.02$ *TeV*, PhysRevLett.116.132302

[16] the ALICE collaboration, *J/ψ suppression at forward rapidity in Pb-Pb collisions at* $\sqrt{s_{\rm NN}} = 5.02$ *TeV*, arXiv:nucl-ex/1606.08197

[17] Shen, Chun and Heinz, Ulrich, *Collision Energy Dependence of Viscous Hydrodynamic Flow in Relativistic Heavy-Ion Collisions*, PhysRev C85.054902

[18] McDonald, Scott and Shen, Chun and Fillion-Gourdeau, Francois and Jeon, Sangyong and Gale, Charles , *Hydrodynamic Predictions for Pb+Pb Collisions at 5.02 A TeV* , arXiv:hep-ph/160902958

[19] Andronic, A. and Braun-Munzinger, P. and Redlich, K. and Stachel, J. *The statistical model in Pb-Pb collisions at the LHC*, Nucl.Phys A905-905.535c

[20] Ferreiro, E. G.,*Charmonium dissociation and recombination at LHC:Revisiting comovers*, Phys.Lett.B731.57

[21] Zhao, Xingbo and Rapp, Ralf, *Medium Modifications and Production of Charmonia at LHC*

[22] Du, Xiaojian and Rapp, Ralf, *Sequential Regeneration of Charmonia in Heavy-Ion Collisions*, Nucl.Phys.A943.145

[23] Zhou, Kai and Xu, Nu and Xu, Zhe and Zhuang, Pengfei, *Medium effects on charmonium production at ultrarelativistic energies available at the CERN Large Hadron Collider*, Phys.Rev.C89.054911